9 January 1998

ELSEVIER

Chemical Physics Letters 282 (1998) 187–191

CHEMICAL PHYSICS LETTERS

Energetics and structures of fullerene crop circles

Jie Han

NASA Ames Research Center, T27A-1, Moffett Field, CA 94035, USA

Received 18 June 1997; in final form 24 October 1997

Abstract

The energetics and structures of carbon tori are studied using molecular simulation. They include circular and polygonal tori, formed by bending (n, n) tubes and by joining (n, n) and $(n+1,\ n-1)$ or $(n+2,\ n-2)$ tubes with pentagon–heptagon defects, respectively, in which $n = 5$, 8 and 10. The strain energy of a circular and polygonal torus decreases by D^{-2} and D^{-1}, respectively, where D is the torus diameter. Comparisons in average and local maximum strain suggest that defect-free circular tori are more energetically stable and kinetically accessible than defective polygonal tori. This confirms the hypothesis that circular tori are the predominant constituents of the observed fullerene crop circles in laser-grown single-wall carbon nanotubes. © 1998 Elsevier Science B.V.

1. Introduction

Fullerene crop circles have been observed in single-wall carbon nanotubes (SWNTs) grown by laser vaporization (LV) method by Liu et al. [1]. These circular structures, with diameters of 90–1000 nm and widths of 1–15 nm, are believed to consist of individual SWNT tori with a tube diameter of ~ 1.0 nm. The toroidal SWNTs are of great interest because of their abundance in $(10, 10)$ metallic nanotubes [2–4]. They could be ideal systems for studying interesting electronic, magnetic and even superconductivity properties in perfectly circular quantum wires. However, the formation and structures of toroidal SWNT require further exploration. It appears that there are no topological pentagon–heptagon defects in these structures as one does not observe obvious kinks that would be created by these defects. This suggests that the torus be formed by bending a straight tube with growing tube eating its own tail [1].

However, the circular appearance of the toroidal nanotubes as seen from transmission electron micrograph (TEM) is not sufficient to rule out the existence of topological pentagon–heptagon defects. Helically coiled multi-wall nanotubes (MWNTs) have been frequently observed during their growth by catalytic decomposition of hydrocarbon and are attributed to the formation of the pentagon–heptagon defects [5,6]. The model suggested for turning tubes on the catalyst particles [5,6] may not apply to SWNT tori prepared by LV method. This is because the nanotube growth mechanisms for the two approaches are different [7]. Toroidal nanotubes formed by introducing the pentagon–heptagon defects have been hypothesized. These structures are not circular, but polygonal with 6- or 5-fold rotational symmetry and 12 or 10 straight nanotube sections making up the toroidal perimeter [8–15]. Their energetics and structures have been studied via computer simulations of small systems (< 2000 atoms or 6 nm in diameter) [8–16]. The proposed polygonal tori, how-

PII S0009-2614(97)01267-0

ever, are pronounced different from the observed circular SWNT tori in, at least, toroidal features.

In this work, Tersoff–Brenner many-body chemical bonding potential [17] is used to study the energetics and structures of circular and polygonal tori of SWNTs. The empirical potential has been shown to be accurate for straight and toroidal carbon nanotubes as compared to first-principles calculations [16]. In addition, it is also computationally feasible to use this potential in studying nanotubes with up to 30000 atoms and torus with diameters up to 60 nm.

2. Circular tori

The circular tori are constructed by bending (n, n) tubes with $n = 5$, 8 and 10 (tube diameter, $d \approx 0.7$, 1.1 and 1.4 nm), respectively. The laser-grown SWNTs in which the fullerene crop circles have been observed consist in a large fraction of $(10, 10)$ metallic tubes [2]. According to the 'scooter' growth mechanism for the LV approaches, the transition metal that co-condenses with the vaporized carbon should prevent the introduction of pentagon defects [2]. Therefore, it is likely that defect-free circular tori form as opposed to defective polygonal tori.

I elucidate the minimum radius of curvature to which SWNTs can be bent and form energetically stable circular tori. I obtain strain–diameter relationships shown in Fig. 1 by energy minimization procedures with the energy gradient, 0.001 eV atom^{-1} Å^{-1} as convergent criterion. The tori consist in 2000 to 30000 atoms. The strain energy is defined as the difference in binding energy between the torus and the straight infinite length tube mimicked by periodic boundary conditions. The torus radius is the averaged distance between all the atom positions and torus center of mass. As expected, the strain energy decreases with the torus diameter. Several featured configurations are shown in Fig. 2 and also can be clearly identified from Fig. 1 using torus $(8, 8)$ as an example. When 8 nm $< D <$ 16 nm, the toroidal tube is buckled and unstable. No energy minima are found as energy gradients are oscillatory around 0.03–0.10 eV atom^{-1} Å^{-1} and the buckling positions keep migrating. The migration is due to existence of a number of small barriers corresponding to kinks. The energy values in this case shown in Fig. 1

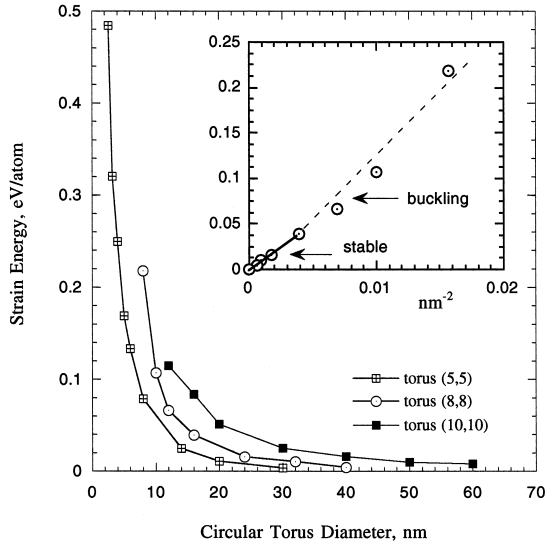

Fig. 1. Strain energy per atom of circular tori relative to straight tubes as functions of torus diameter, D. The insert shows a linear relation between the strain energy and D^{-2} for stable torus $(8, 8)$. The turning point represents a transition from buckling to stable states. Reference energy is -7.2513, -7.3231 and -7.3482 eV atom^{-1} for straight infinite length tube $(5, 5)$, $(8, 8)$ and $(10, 10)$, respectively.

are the averages over period of oscillation. As the torus diameter increases, the bending strain is alleviated and buckling disappears. The torus becomes energetically stable when $D >$ 16 nm. However, the tube cross section of the stable torus changes from an ellipse with major axis perpendicular to the torus plane to circle. When strain energy < 0.03 eV atom^{-1}, the tube cross section is circular (the ratio of major to minor axis < 1.1) and the local maximum strain, the difference between the energy maxima at atom positions of the torus and the energy of corresponding straight tube, is less than 1.1 times the averaged strain. This is a common feature to all the three types of tori. Thus, I prefer calling the torus with circular tube cross section the perfect circular torus. In a perfect circular torus, strain can be considered to be evenly distributed over all the atoms. The diameters to reach this state are approximately 15, 25 and 40 nm for torus $(5, 5)$, $(8, 8)$ and $(10, 10)$, respectively. When diameter increases to 100 nm, the strain energy is estimated to be less than 0.01 eV atom^{-1} for torus $(10, 10)$.

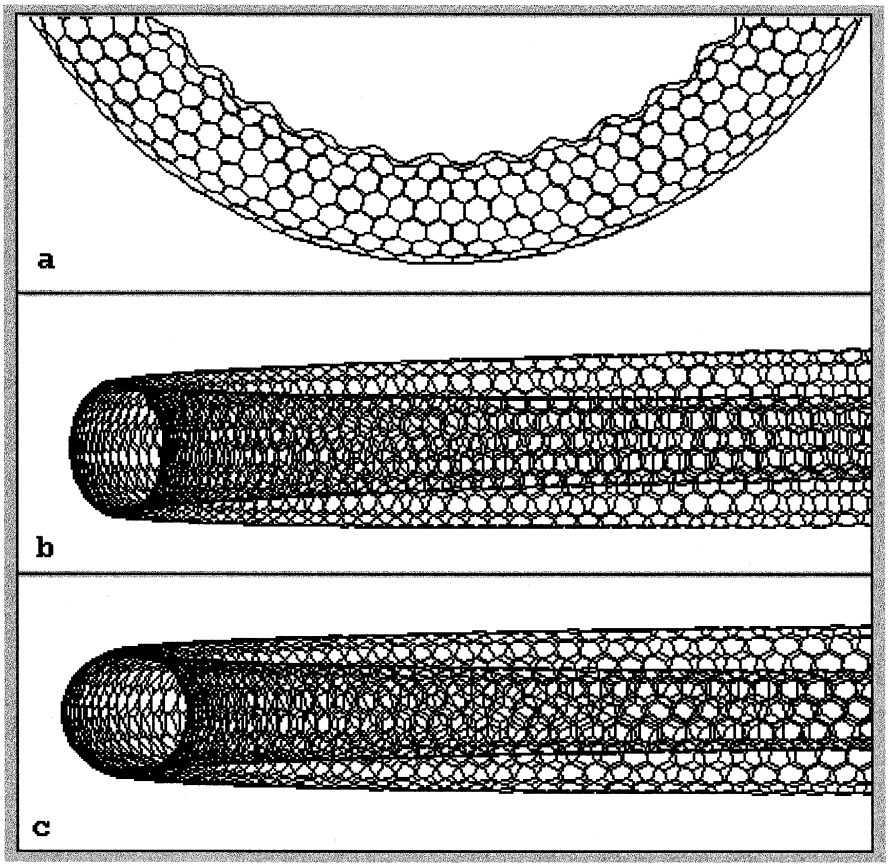

Fig. 2. Configurations of circular torus (8, 8). As torus diameter increases, the tube cross section changes from (a) buckling to (b) ellipse and to (c) circle.

It is well known the tube strain energy per atom relative to the graphene sheet is proportional to d^{-2} [18]. This work indicates that the strain energy per atom of stable torus relative to the straight tube is D^{-2} dependent (see the insert in Fig. 1). Therefore, from the energetic point of view, bending a straight tube is similar to bending a planar sheet. Beyond the elastic limit of tube, bending leads to buckling. The critical diameter for buckling were found to be ~ 6, 16 and 30 nm for torus (5, 5), (8, 8) and (10, 10), respectively. Iijima et al. have derived a correlation between tube diameter ($d = 1$–1.5 nm) and the critical curvature at which bending leads to buckling [19]. Their results are ~ 8.5 and 14.0 nm as the critical buckling radius for tube (8, 8) and (10, 10), respectively, in agreement with my values (~ 8 and 15 nm) for tube buckling in circular torus (8, 8) and (10, 10).

3. Polygonal tori

For comparison with circular tori, I also studied polygonal tori formed by joining (n, n) and $(n + 1, n - 1)$ or $(n + 2, n - 2)$ tube sections with topological pentagon–heptagon defects since they look more like circular tori than previously proposed polygonal tori with 5- or 6-fold rotation symmetry [8–15]. An example is illustrated in Fig. 3 where a torus is formed by 30-fold rotation of joint (5, 5)/(6, 4)/(5, 5). In this work, a joint geometry was optimized and then the optimized bent angle was adjusted slightly to such a value that 360° was

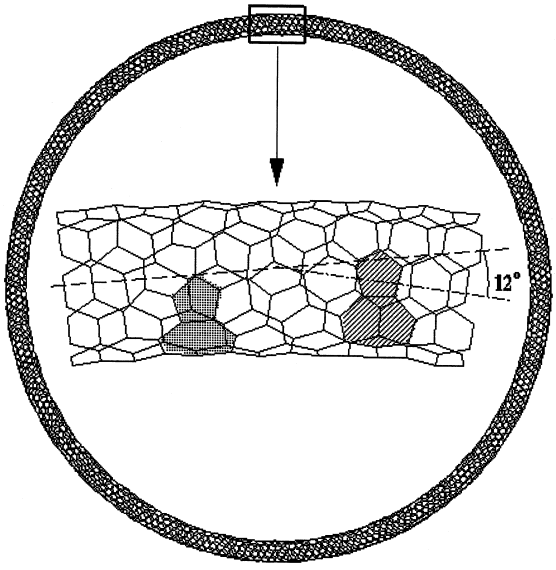

Fig. 3. Polygonal tori formed by a 30-fold rotation of the $(5,5)/(6,4)/(5,5)$ joint unit with bent angle of 12°. Note that two pairs of fused pentagon–heptagon defects are in opposed sides.

its integer multiple in order to rotate this joint into a polygonal tori. The bent angle and the number of defects are 12° and 60, 36° and 40, and 9° and 90 for torus constructed by joint $(5,5)/(6,4)/(5,5)$, $(5,5)/(7,3)/(5,5)$ and $(10,10)/(11,9)/(10,10)$ with one, two and one fused pentagon–heptagon defect pairs, respectively. The small angle joints with fused pentagon–heptagon pairs were also proposed for $(7,1)/(8,0)$ and $(5,3)/(8,0)$ by Chico et al. [20] in contrast to Dunlap's 30° joints with separated defects [8].

The strain energies for these three polygonal tori are shown in Fig. 4. The reference energy and measure of torus diameter are the same as for the circular tori. The torus diameter varies by changing the length of straight tube. The total strain energy of a polygonal torus is proportional to the total number of the defects while the strain per atom is proportional to $1/N$ (N, number of atoms) or $1/D$ if the tube bending strain is ignored. Thus two features can be seen from Fig. 4. The strain energy for the same tube diameter is lowered from torus $(6,4)/(5,5)$ (60 defects) to $(7,3)/(5,5)$ (40 defects). On the other hand, the strain energy of a polygonal torus, for example, $(7,3)/(5,5)$, is lower in the range of small diameters and higher in the larger diameters than that of circular torus, for example, $(5,5)$. This is because the strain energy per atom is proportional to D^{-2} for the circular tori and D^{-1} for the polygonal tori (see the insert in Fig. 4). The observation that the strain energy of a polygonal torus is a linear function of D^{-1} implies that the tube bending ($\sim D^{-2}$) can be ignored compared to dominant contribution of the defects to the total strain in the polygonal tori. In general, the strain energy of a polygonal torus jointing (n, n) and $(n+1,\ n-1)$ or $(n+2,\ n-2)$ tube segments is larger than that of a perfect circular torus (n, n) although lower strain of polygonal tori relative to circular tori can be reached for smaller torus diameters.

The averaged strain per atom will be zero for both circular and polygonal tori if D goes to infinity. For circular tori, this means that strain disappears both globally and locally since the strain is evenly distributed. For polygonal tori, however, the defect strain is independent of diameter and will not vanish. Therefore, the averaged strain per atom is not a sufficient measure and the local maximum strain should be considered. The local maximum strain was found to be 0.13 eV atom^{-1} for the $(6,4)/(5,5)$ torus, localized at one pentagon–heptagon defect and 0.21 eV atom^{-1} for the $(7,3)/(5,5)$ torus, localized

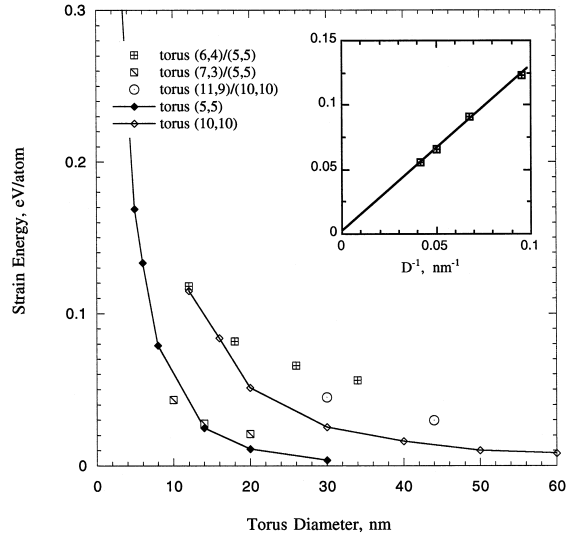

Fig. 4. Strain energy per atom of tori relative to straight tubes as function of torus diameter, D. The insert shows a linear relation between the strain energy and D^{-1} for polygonal torus $(6,4)/(5,5)$.

at two pentagon–heptagon defects. It changed slightly to 0.11 eV atom^{-1} for the $(11,9)/(10,10)$ torus. These values are much higher than those for perfect circular tori.

4. Concluding remarks

I carried out systematic molecular mechanics calculations for circular and polygonal tori. The total and local maximum strain energy results indicate a preference for perfect circular tori over polygonal tori although both are energetically stable for torus diameter over certain critical values. This confirms the hypothesis that defect-free circular SWNT tori are the predominant constituents of the observed crop circles in laser-grown SWNTs [1].

The strain energy per atom is not sufficient for the identification of stable carbon cage structures if the strain distributions are not evenly distributed over all the atoms. Therefore, I added the local maximum strain as an indicator of the kinetic energy barrier to the local structure formation for this purpose. The strain energy per atom relative to graphite is higher for C_{60} than C_{70} and higher fullerenes [21]. However, C_{60} has highest stability from both kinetic and energy point of view. This is because the strain energy is most evenly distributed over each atom and the local maximum strain is the lowest for the highest-symmetry C_{60} compared to all the fullerenes. Similarly, circular tori are more energetically stable and kinetically accessible than polygonal tori because the total strain or local maximum strain in a circular torus is evenly distributed and gets effectively released as the bent tube is lengthened. The previous studies comparing only strain energy per atom relative to C_{60} for evaluations of relative stability of carbon cage structures including polygonal tori might be not sufficient.

I also wish to emphasize that the preference of circular tori over defective polygonal tori in this work is specific for the laser-grown SWNTs. In fact, defective tube joints have been believed to be responsible for the formation of observed helically coiled MWNTs on catalyst particles in which coil radius can be as small as 16 nm with a tube diameter > 2 nm [5,6]. My calculations show that a tube with diameter at 1.4 nm cannot be bent to form stable coil with radius < 20 nm. This rules out possibility of the helically coiled structure being formed by bending a nanotube without introducing topological defects. The survived defects could be related to Van der Waals interactions between tube walls and between tube wall and catalyst particles. If catalysts do stabilize the topological pentagon–heptagon defects, it is likely that joint structures from the catalyst particle-grown SWNTs will be observed.

Acknowledgements

I gratefully acknowledge Dr. Hongjie Dai and Dr. Richard Jaffe for discussions and suggestions. This work is supported by Director's Discretionary Fund and MRJ, Inc. at NASA Ames Research Center through contract NAS2-14303.

References

[1] J. Liu, H. Dai, J.H. Hafner, D.T. Colbert, S.J. Tans, C. Dekker, R.E. Smalley, Nature (London) 385 (1997) 780.
[2] A. Thess, R. Lee, P. Nikolaev, H. Dai, P. Petit, J. Robert, C. Xu, Y.H. Lee, S.G. Kim, D.T. Colbert, G. Scuseria, D. Tomanek, J.E. Fischer, R.E. Smalley, Science 273 (1996) 483.
[3] J.E. Fischer, H. Dai, A. Thess, R. Lee, N.M. Hanjani, D. DeHaas, R.E. Smalley, Phys. Rev. B 55 (1997) 4921.
[4] S.J. Tans, M.H. Devoret, H. Dai, A. Thess, R.E. Smalley, L.J. Geerlings, C. Dekker, Nature (London) 386 (1997) 474.
[5] S. Amelinckx, X.B. Zhang, D. Bernaerts, X.F. Zhang, V. Ivanov, J.B. Nagy, Nature (London) 265 (1994) 635.
[6] X.F. Zhang, Z. Zhang, Phys. Rev. B 52 (1995) 5313.
[7] H. Dai, A. Rinzler, P. Nikolaev, A. Thess, D.T. Colbert, R.E. Smalley, Chem. Phys. Lett. 260 (1996) 471.
[8] B.I. Dunlap, Phys. Rev. B 46 (1992) 1933.
[9] L.A. Chernozatonskii, Phys. Lett. A 170 (1992) 37.
[10] S. Itoh, S. Ihara, J. Kitakami, Phys. Rev. B 47 (1993) 1703.
[11] S. Itoh, S. Ihara, J. Kitakami, Phys. Rev. B 48 (1993) 5643.
[12] S. Itoh, S. Ihara, J. Kitakami, Phys. Rev. B 48 (1993) 5643.
[13] S. Itoh, S. Ihara, Phys. Rev. B 48 (1993) 8323.
[14] S. Itoh, S. Ihara, Phys. Rev. B 49 (1994) 13970.
[15] B. Borstnik, D. Lukman, Chem. Rev. Lett. 228 (1994) 312.
[16] J.K. Johnson, B.N. Davidson, M.R. Pederson, J.Q. Broughton, Phys. Rev. B 50 (1994) 17575.
[17] D.W. Brenner, Phys. Rev. B 42 (1990) 9458.
[18] D.H. Robertson, D.W. Brenner, J.W. Mintmire, Phys. Rev. B 45 (1992) 12593.
[19] S. Iijima, C. Brabec, A. Maiti, J. Bernholc, J. Chem. Phys. 104 (1996) 2089.
[20] L. Chico, V.H. Crespi, L.X. Benedict, S.G. Louie, M.L. Cohen, Phys. Rev. Lett. 76 (1996) 971.
[21] A. Maiti, C.J. Brabec, J. Bernholc, Phys. Rev. Lett. 70 (1993) 3023.